Dielectric properties of Mn doped ZnO nanostructures

S. Ajin Sundar, N. Joseph John

Abstract— **Zinc oxide and Mn doped zinc oxide nanoparticles were synthesized by wet chemical technique using zinc acetate dehydrate as a precursor. Highly stable pure and 0.2, 0.4, 0.6, 0.8, 1.0 and 5.0 weight percentage Mn doped ZnO nanoparticles have been prepared at room temperature. The detailed structural properties were examined using X-ray diffraction pattern (XRD) which revealed that the synthesized nano particles are well crystalline and possessing wurtzite hexagonal phase. The dielectric studies were carried out. The present study indicates that the polarization mechanism in the nano particles considered is mainly contributed by space charge polarization. It can be understood that the space charge contribution plays an important role in the charge transport and polarizability in all the systems considered in the present study. The dielectric constant, dielectric loss, AC conductivity and DC conductivity increases with increase in temperature.**

Index Terms— **AC conductivity, DC conductivity, dielectric constant, dielectric loss, Nanoparticles, X-ray techniques.**

I. INTRODUCTION

Zinc oxide (ZnO) is a wide band gap semiconductor with wurtzite structure. The physical and chemical properties of nano scale particles are different when compared with the bulk materials. Nano powders contolled to nanocrystalline size can show atom like behavior which results from higher surface energy. It is due to the large surface area and wider band gap between the conduction and valence band [1]. It is an n-type direct band gap group II–VI semiconductor material, has received a great deal of attention for its use in various fields . Due to its high optoelectronic efficiencies relative to the indirect band gap group IV crystals, its wide band gap (3.37 eV), high exciton binding energy (E60 meV), and high dielectric constant, ZnO is considered as an important material for variety of applications in the visible and near ultraviolet regions [2, 3]. Nanometer-size zinc oxide has many new exciting properties and wide technological applications such as photocatalysis, chemical remediation, photoinitiation of polymerization reactions, quantum dot devices, solar energy conversion, biochemical sensors, chemical electrode, cosmetics, and pigments [4–13]. Furthermore, ZnO nanoparticles also have good biocompatibility to human cells [14] and their antibacterial and antifungal activities have been already demonstrated [15, 16]. ZnO has exhibited various kinds of nanostructures

S. Ajin Sundar, Department of Physics, Government Arts College, Udhagamandalam, Tamilnadu, India. Pin – 643 002. Mobile : 9488081236,

N. Joseph John, Department of Physics, Sethupathy Government Arts College, Ramanathapuram, Tamilnadu, India. Pin-623502. Mobile : 9487116671

including nanoneedles, nanobelts, nanoflowers, nanorods, nanobows, nanonails, nanoparticles, and nanowires [17].

There are several solution based routes are available for the preparation of ZnO nanoparticles such as solvothermal, hydrothermal, sol-gel, micro-emulsion, vapour phase transport process, precipitation, RF magnetron sputtering, etc.In the present work,an attempt has been made to synthesis ZnO and Mn-doped ZnO nanoparticles by wet chemical method. Zinc oxide due to its versatility and multifunctionality creates attention in the research field related to its applications. A wide number of synthesis techniques also been developed by which ZnO can be grown in different nanoscale forms and thereby different novel nanostructures can be fabricated with different shapes ranging from nanowires to nanobelts and even nanosprings. Many fine optical devices can be fabricated based on the free-exciton binding energy in ZnO that is 60 meV because large exciton binding energy makes ZnO eligible to persist at room temperature and higher too. Since ZnO crystals and thin films exhibit second- and third-order non-linear optical behaviour, it can be used for non-linear optical devices. Third-order non-linear response has recently been observed in ZnO nano crystalline films which make it suitable for integrated non-linear optical devices. Generally, the advantage of tuning the physical property of these oxides like zinc oxide becomes the root cause for the synthesis of smart application device. The electrical, optical, magnetic, and chemical properties can be very well tuned by making permutation and combination of the two basic structural characteristics they possess these cations with mixed valence states, and anions with deficiencies(vacancies). Thus, making them suitable for several application fields such as semiconductor, superconductor, ferroelectrics, and magnetic. DSSCs is an optoelectronics device that converts light to electrical energy via charge separation in sensitizer dyes absorbed on a wide band gap semiconductor, which is different to conventional cells. One important difference between conventional and dry sensitized solar cell is that they are epitomized by silicon p-n junction solar cells. The demand for zinc oxide based dye-sensitized solar cell is due to its low fabrication cost.

II. MATERIALS AND METHODS

Analytical reagent (AR) grade samples of Zinc acetate dehydrate, Sodium hydroxide, and sodium dodecyl sulphate (purchased from Merck, India) along with double distilled water were used for the synthesis of pure ZnO. Manganese chloride ($MnCl_2$) in seven different weight percentages viz 0.0, 0.2, 0.4, 0.6, 0.8,1.0 and 5.0 were dissolved in double distilled water under vigorous stirring till the solution becomes homogeneous. Then zinc acetate dehydrate was added to the solution under stirring, along with it NaOH and Sodium Dodecyl Sulphate were added till pH value reaches

12 and the solution was kept for drying in a hot air oven and heated at 160 °C for overnight. The material was taken and grinded using a mortar and pestle and thus obtained powder was washed several times using ethanol and deionized water. The purpose of washing the product with ethnol was to remove the unwanted salt and impurities. The product was dried at 60°C for two days and obtained product was kept for calcinations at 500°C for four hours.

The crystal structure and phase impurity were analysed using XRD measurements with standard X-ray diffractometer (XPERT-PRO, wavelength 0.154nm). The average crystallite size was determined from XRD peaks using Scherer's formula.The composition of the samples was determined by energy dispersive X-ray spectroscopy using scanning microscope.

The prepared nanocrystals were palletized using a hydraulic press (with a pressure of about 5 tons) and used for the AC electrical measurements. The flat surfaces of the cylindrical pellets were coated with good quality graphite to obtain a good conductive surface layer. Using a traveling microscope the dimensions of the pellets were measured. The capacitance (Cc) and the dielectric loss factor (tan δ) were measured using the conventional parallel plate capacitor method [18-25] using an LCR meter (APLAB 4912) for all the samples with two frequencies 100 Hz and 1 kHz at various temperatures ranging from 30 - 150°C. The observations were made while cooling the sample. The temperature was controlled to an accuracy of ± 1°C. Air capacitance (C_a) was also measured for the thickness equal to that of the pellet. The area of the pellet in contact with the electrode is same as that of the electrode. The air capacitance was measured only at room temperature because the variation of air capacitance with temperature was found to be negligible. The dielectric constant of the pellet sample was calculated using the relation,

$$\varepsilon_r = C_c / C_a.$$

The AC electrical conductivity (σ_{ac}) was calculated using the relation,

$$\sigma_{ac} = \varepsilon_0 \, \varepsilon_r \, \omega \tan \delta.$$

Here, ε_0 is the permittivity of free space (8.85 x 10^{-12} $C^2 N^{-1} m^{-2}$) and ω is the angular frequency ($\omega = 2\pi f$, where f is the frequency).

III. RESULTS AND DISCUSSION

Figure 1 shows the representative XRD pattern of ZnO nanoparticles before and after Mn doping. The eight major peaks were seen at 31.7, 34.6, 36.2, 47.6, 56.5, 62.9, 68.0 and 69.8 which can be assigned to diffraction from (100), (002), (101), (102), (110), (103), (112) and (201) planes respectively. The sharp intense peaks of ZnO confirm the good crystalline nature of ZnO and diffraction peak can be indented to a hexagonal wurtize structured zinc oxide. All these data are in agreement with JCPDS files. There is no indication of any secondary phase or clusters confirming that the samples are only one single phase.
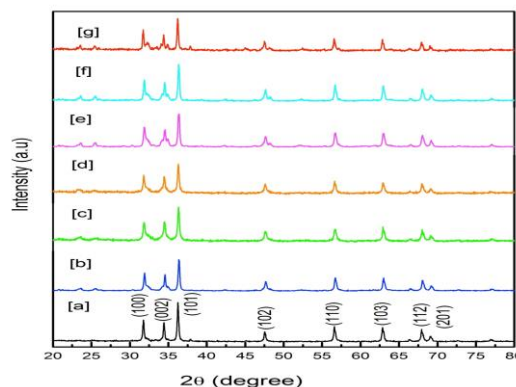

Fig: 1 XRD Spectra for [a] ZnO, [b] 0.2 wt % Mn-ZnO, [c] 0.4 wt% Mn-ZnO, [d] 0.6 wt% Mn-ZnO, [e] 0.8 wt% Mn-ZnO, [f] 1.0 wt% Mn-ZnO, [g] 5.0 wt% Mn-ZnO.

The XRD result also indicate that Mn ions systematically substituted for the Zn ions in the sample without changing the wurtizite structure. The most intense diffraction peak (101) is clearly evident with a slight shift into low angular scale where as the corresponding intensity decreases compared with undoped ZnO. Furthermore the intensity of the diffraction peaks decreases and the width broadens due to the formation of smaller grain diameter as a result of an increase disorder of Mn doping. The average crystalline size obtained from XRD studies were given in Table 1.

Table 1. XRD Average crystallite size.

Sample	Average crystallite size(nm)
Zinc Oxide	40.587
0.2 wt % Mn-ZnO	36.119
0.4 wt % Mn-ZnO	48.510
0.6 wt % Mn-ZnO	57.028
0.8 wt % Mn-ZnO	48.961
1.0 wt % Mn-ZnO	33.182
5.0 wt % Mn-ZnO	43.877

The dielectric parameters viz. ε_r, tan δ and σ_{ac} and σ_{dc} observed are shown in Figures 2-5. All the parameters increase with increase in temperature. The dielectric constant is attributed to four types of polarization which are space charge, dipolar, ionic and electronic [26].
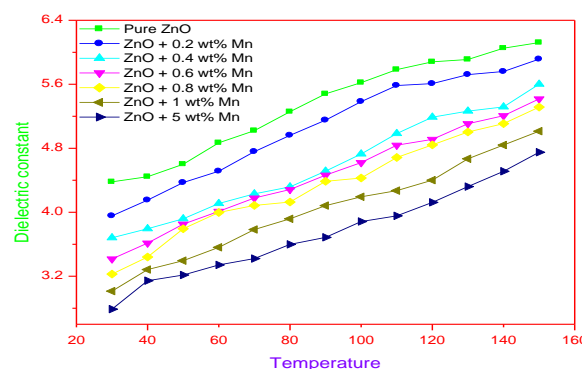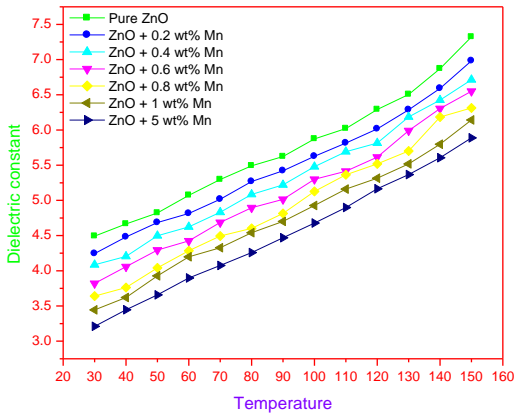
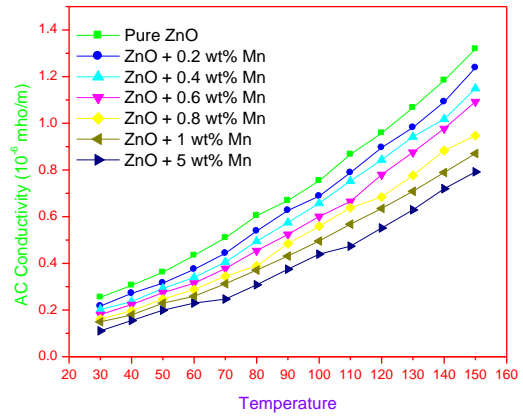Fig 2: Variation of dielectric constant with temperature (a) at 100 Hz (b) 1KHz

Fig 3: Variation of dielectric loss with temperature (a) at 100 Hz (b) 1KHz

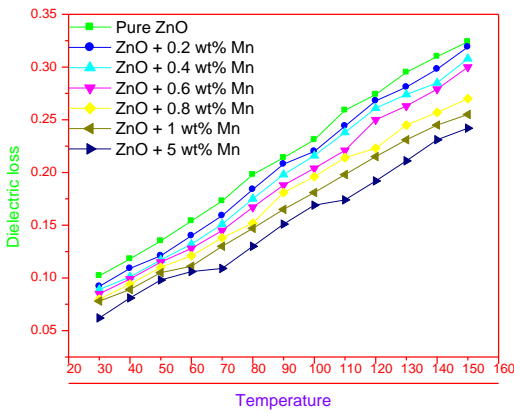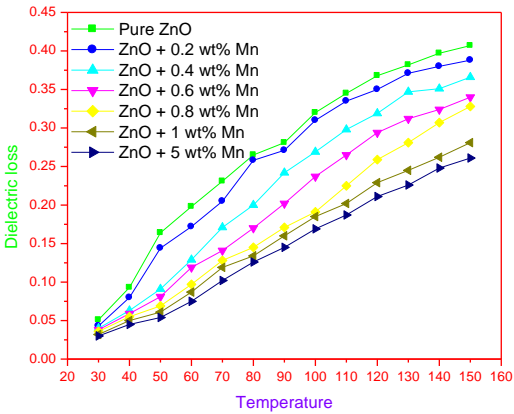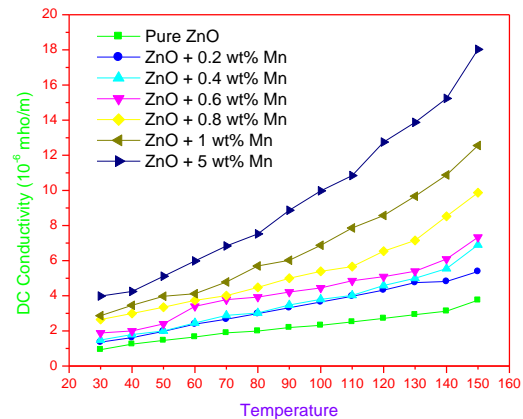Fig 4: Variation of AC conductivity with temperature (a) at 100 Hz (b) 1KHz

Fig 5: Variation of DC conductivity with temperature

At lower frequencies at which all four types of polarizations contribute, the rapid increase in dielectric constant is mainly due to space charge and dielectric polarizations, which are strongly temperature dependent[26,27].

In the case of space charge polarization which is due to the accumulation of charges at the grain boundary, an increase in polarization results as more and more charges accumulate at the grain boundary with the increase in temperature. Beyond a certain temperature, the charges acquire adequate thermal energy to overcome the resistive barrier at the grain boundary and conduction takes place resulting in decreasing of polarization. This interfacial polarization occurs up to frequency at 1 kHz with possibly some contribution from the dipolar polarization also as the temperature increases. The grain size observed for the two systems considered in the present study are less than 58 nm. So it can be understood that the polarization mechanism is mainly contributed by the space charge polarization. Nanoparticles lie between the infinite solid state and molecules. The electrical resistivity of nanocrystalline material is higher than that of both conventional coarse grained polycrystalline materials alloys. The magnitude of electrical resistivity and hence the conductivity in composites can be changed by altering the size of the electrically conducting component. The σ_{ac} values observed in the present study are very small. When the grain size is smaller than the electron mean free path, grain

boundary scattering dominates and hence electrical resistivity is increased. Thus the space charge contribution plays an important role in the charge transport process and polarizability in the case of all the systems considered in the present study.

IV. CONCLUSION

Pure ZnO and the transition metal manganese doped at various weight percentage were successfully synthesized by using zinc acetate dihydrate as a precursor using wet chemical technique. The prepared nanoparticles were characterized by XRD. The XRD measurement suggests that Mn atoms substitute Zn sites without changing the hexagonal wurtize structure. The dielectric parameters increase with increase in temperature. The results obtained indicate that the space charge contribution plays an important role in the charge transport process and polarizability.

REFERENCES

[1] Y. Nakayama, P. J. Pauzauskie, A. Radenovic et al., "Tunable nanowire nonlinear optical probe," *Nature*, vol. 447, no. 7148, pp. 1098–1101, 2007.

[2] C. F. Lin, W. Y. Su, and J. S. Huang, "Improving the property of ZnO nanorods using hydrogen peroxide solution," *Journal of Crystal Growth*, vol. 310, no. 11, pp. 2806–2809, 2008.

[3] S. H. Yu and H. Cölfen, "Bio-inspired crystal morphogenesis by hydrophilic polymers," *Journal of Materials Chemistry*, vol. 14, no. 14, pp. 2124–2147, 2004.

[4] Y. Li, K. Wu, and I. Zhitomirsky, "Electrodeposition of composite zinc oxide-chitosan films," *Colloids and Surfaces A*, vol. 356, no. 1–3, pp. 63–70, 2010.

[5] S. I. Na, S. S. Kim, W. K. Hong et al., "Fabrication of TiO2 nanotubes by using electrodeposited ZnO nanorod template and their application to hybrid solar cells," *Electrochimica Acta*, vol. 53, no. 5, pp. 2560–2566, 2008.

[6] M. F. Hossain, T. Takahashi, and S. Biswas, "Nanorods and nanolipsticks structured ZnO photoelectrode for dye-sensitized solar cells," *Electrochemistry Communications*, vol. 11, no. 9, pp. 1756–1759, 2009.

[7] W. Chen, H. Zhang, I. M. Hsing, and S. Yang, "A new photoanode architecture of dye sensitized solar cell based on ZnO nanotetrapods with no need for calcination," *Electrochemistry Communications*, vol. 11, no. 5, pp. 1057–1060, 2009.

[8] W. Sun, Z. Zhai, D. Wang, S. Liu, and K. Jiao, "Electrochemistry of hemoglobin entrapped in a Na□on/nano-ZnO film on carbon ionic liquid electrode," *Bioelectrochemistry*, vol. 74, no. 2, pp. 295–300, 2009.

[9] J. Singh, J. Im, J. E. Whitten, J. W. Soares, and D. M. Steeves, "Chemisorption of a thiol-functionalized ruthenium dye on zinc oxide nanoparticles: implications for dye-sensitized solar cells," *Chemical Physics Letters*, vol. 497, no. 4–6, pp. 196–199, 2010.

[10] C. Xiang, Y. Zou, L. X. Sun, and F. Xu, "Direct electrochemistry and enhanced electrocatalysis of horseradish peroxidase based on fowerlike ZnO-gold nanoparticle-Na□on nanocomposite," *Sensors and Actuators B*, vol. 136, no. 1, pp. 158–162, 2009.

[11] X. Liu, Q. Hu, Q. Wu, W. Zhang, Z. Fang, and Q. Xie, "Aligned ZnO nanorods: a useful □lm to fabricate amperometric glucose biosensor," *Colloids and Surfaces B*, vol. 74, no. 1, pp. 154–158, 2009.

[12] G. Zhao, J. J. Xu, and H. Y. Chen, "Interfacing myoglobin to graphite electrode with an electrodeposited nanoporous ZnO film," *Analytical Biochemistry*, vol. 350, no. 1, pp. 145–150, 2006.

[13] J. Zhao, J. Zhi, Y. Zhou, and W. Yan, "A tyrosinase biosensor based on ZnO nanorod clusters/nanocrystalline diamond electrodes for biosensing of phenolic compounds," *Analytical Sciences*, vol. 25, no. 9, pp. 1083–1088, 2009.

[14] N. Padmavathy and R. Vijayaraghavan, "Enhanced bioactivity of ZnO nanoparticles—an antimicrobial study," *Science and Technology of Advanced Materials*, vol. 9, no. 3, Article ID 035004, 2008.

[15] L. He, Y. Liu, A. Mustapha, and M. Lin, "Antifungal activity of zinc oxide nanoparticles against *Botrytis cinerea* and *Penicillium expansum*," *Microbiological Research*, vol. 166, no. 3, pp. 207–215, 2011.

[16] S. A. Ansari, Q. Husain, S. Qayyum, and A. Azam, "Designing and surface modi□cation of zinc oxide nanoparticles for biomedical applications," *Food and Chemical Toxicology*, vol. 49, no. 9, pp. 2107–2115, 2011.

[17] A. E□ekhari, F. Molaei, and H. Arami, "Flower-like bundles of ZnO nanosheets as an intermediate between hollow nanosphere and nanoparticles," *Materials Science and Engineering A*, vol. 437, no. 2, pp. 446–450, 2006.

[18] P. Sivakala, N. Joseph John and S. Perumal "Investigation on the Growth and Physio-Chemical Properties of L-Alanine Mixed BTCBC Single Crystals" *Int. res. J. Eng. And Tech., 3,2,2016* , 987-991.

[19] P. Sivakala, N. Joseph John and S. Perumal "Investigation on the Growth and Physio-Chemical Properties of L-Alanine Mixed BTCBC Single Crystals" *Int. Journal of Engineering Research and Applications, Vol. 4, Issue 7(Version 4), July 2014, pp.145-151.*

[20] Jayaprakash Manoharan A. J., Joseph John N., Andavan P. " Effect of amino acid doping on the dielectric properties of triglycine sulphate (TGS) single crystals", Ind. J. of Sci. and Tech., 4,6, 2011, 688-691.

[22] Jayaprakash Manoharan A. J., Joseph John N., Andavan P. "Dielectric properties of proline doped Triglycine sulphate (TGSP) crystals, Journal of Experimental Sciences, (2011) , 2(2), 33-35.

[23] Joseph John N., Selvarajan P., Mahadevan C. K. "Growth, Structural, Optical, Mechanical and Dielectric Characterization of Diammonium Hydrogen Phosphate (DAHP) single Crystals", Journal of Minerals and Material characterization and Engineering, (2011), 10, 15, 1379-1389.

[24] Joseph John N., Selvarajan P., Mahadevan C. K. "Studies on NaCl added ADP single crystals " Materials and Manufacturing Processes (2008) 23, 809-815.

[25] Joseph John N., Selvarajan P., Mahadevan C. K., "Growth and characterization of disodium hydrogen phosphate (DSHP) single crystals" , Materials and Manufacturing Processes (2007) 22, 379-383.

[26] L.C. Hench and J.K. West (1990) Principles of Electronic Ceramics [John Wiley and sons , NewYork]

[27] A.Verma, O.P.Takur, C.Prakash, T.C. Goel and R.G. Mendrinatta, "Temperature dependence of electrical properties of nickel–zinc ferrites processed by the citrate precursor technique" Mater.Sci. Engg. B 116, 1, 1-6 (2005).